International Journal of Mass Spectrometry 292 (2010) 7–13

Contents lists available at ScienceDirect

International Journal of Mass Spectrometry

journal homepage: www.elsevier.com/locate/ijms

Electron impact total ionization cross sections for halogens and their hydrides

Minaxi Vinodkumar[a], Rucha Dave[b], Harshad Bhutadia[a], Bobby K. Antony[c,*]

[a] V.P. & R.P.T.P. Science College, Vallabh Vidyanagar, 388120, Gujarat, India
[b] Anand Agricultural University, Anand 388110, Gujarat, India
[c] Department of Applied Physics, Indian School of Mines, Dhanbad, JH-826004, India

ARTICLE INFO

Article history:
Received 18 October 2009
Received in revised form 11 February 2010
Accepted 11 February 2010
Available online 18 February 2010

PACS:
34.50.−s
34.80.Bm
34.50.Gb

Keywords:
Halogen
Halogen hydrides
Ionization cross sections
Excitation cross sections
Complex spherical optical potential
Complex scattering potential-ionization contribution

ABSTRACT

Calculation for electron impact total ionization cross sections on halogen atoms (F, Cl, Br and I) and their hydrides (HF, HCl, HBr and HI) are performed employing Spherical Complex Optical Potential and Complex Optical Potential-ionization contribution formalisms. In this article we are presenting data for energies ranging from above threshold to 2000 eV. Our results are compared with available experimental and theoretical data wherever available. It is found that the present result gives a better account of the ionization cross sections.

1. Introduction

Electron scattering by halogens are a major concern in low temperature plasma, especially in technologies like fusion reactors, gas discharges, semiconductor etching, mass spectrometry and astrophysics [1]. Knowledge of reliable collision cross section is imperative in modeling plasmas in these environments. The accuracy of such modeling depends largely on ionization cross section data. Because of their importance to industrial plasma, many studies have been conducted on these atoms and molecules. However, the experimental database for these targets seems to be fragmented and incomplete may be due to their highly reactive nature. Hence, a reliable calculation like Spherical Complex Optical Potential (SCOP) method [2–4] could effectively fill the gap in the required database. Besides, the availability of cross section data for the halogen atoms offer a direct prospect of comparing data with the neighboring rare gases and thus helping to refine our method to predict results for more targets which have not been studied earlier.

There are handful experimental studies on halogen atoms and none in case of total or partial ionization cross sections of halogen hydrides till date to the best of our knowledge. One of the earliest ionization cross section measurements for halogen atoms is reported by Hayes et al. [5]. However, they have presented the result with accuracy less than 20%, which is quite low for using it for further modeling. In 1990, Freund et al. [6] have reported the ionization cross section measurements for many atomic targets using a crossed-electron-beam–fast-atom-beam method using the same apparatus used by Hayes et al. [5]. The systematic uncertainty for this arrangement is claimed to be 10%, which is quite good. Ali and Kim [7] recently reported theoretical data for halogen atoms Br and I, diatomic halogens Br_2 and I_2 as well as for their hydrogen halides HCl, HBr and HI. A comprehensive calculation for all atoms from hydrogen to uranium on the basis of semi-classical approach (more popularly known as DM or Deutsch–Märk formalism) is reported by Margreiter et al. [8]. Joshipura and Limbachiya [9] have also reported theoretical data on total ionization cross section data for atomic and molecular halogens. They have also used SCOP method; however, present Complex Optical Potential-ionization contribution (CSP-ic) method uses a dynamic energy dependant ratio to extract Q_{ion} from Q_{inel}, which gives a better representation of the target and thereby producing improved results. Finally, Huo [10] reported total ionization cross sections for Cl, Br and I using the effective core potential orbital from threshold to 1000 eV.

* Corresponding author. Tel.: +91 9470194795.
E-mail address: bka.ism@in.com (B.K. Antony).

1387-3806/$ – see front matter © 2010 Elsevier B.V. All rights reserved.
doi:10.1016/j.ijms.2010.02.009

The case of halogen hydrides is worse in the sense that there is no experimental data and there is paucity for theoretical data too. There are no measurements available for these species may be due to their high volatile nature and hence, difficult in performing experiments. For HF, HCl and HBr we could find theoretical data reported by Deutsch et al. [11] which is available for limited energy range between 30 and 150 eV. They used modified additivity rule for calculating total ionization cross sections. For HF, the sample results were predicted by Fitch and Sauter [12] and Bobeldijk et al. [13] using the additivity rule. More recent calculations on all above listed halogen hydrides except HF were done by Ali and Kim [7] and due to the paucity of both theoretical and experimental data for these targets; they have compared their data using two different methods viz. Binary Encounter Bethe (BEB) method and Effective Core Potentials (ECP) method as suggested by Huo and Kim [14]. In ECP method, the potentials are developed solely on the coordinates of the valence electrons, thereby eliminating the need for the core basis functions which usually require a large set of Gaussians to describe them. Electron impact total ionization cross section for HI is calculated only by Ali and Kim [7].

Presently we have made use of the well-established Complex Optical Potential (SCOP) [15–17] formalism to obtain the total ionization cross sections discussed here. The methodology employed is discussed in the next section depicting the salient features of the theory. A more detailed description can be found in our earlier papers [18,19].

2. Theoretical methedology

Total ionization cross section (Q_{ion}) upon electron impact for the halogens and their hydrides are calculated using SCOP formalism as mentioned in the previous section. The present theory is based on a quantum mechanical calculation solved by the method of partial waves, giving complex phase shifts as the output. The phase shift thus obtained is the key ingredients and they carry the signature of the interaction of the incoming projectile and the target. These phase shifts are further used to evaluate the total elastic cross sections (Q_{el}) and its inelastic counterpart (Q_{inel}) [20] such that

$$Q_T(E_i) = Q_{el}(E_i) + Q_{inel}(E_i) \tag{1}$$

However, our objective in this study is restricted to the calculation of the Q_{ion} for halogens and their hydrides, since this cross section is central to many applications related to plasma and other technologies mentioned in the introduction. Ionization is the predominant scattering process in the inelastic channel for incident electron energy ranging from ionization threshold to about 2 keV. Hence, we have limited our calculation to this energy where channels that lead to discrete as well as continuum transitions in the target are open.

We represent the electron–atom/molecule system by a complex potential comprising of real and imaginary potentials as

$$V(r, E_i) = V_R(r, E_i) + iV_I(r, E_i) \tag{2}$$

such that

$$V_R(r, E_i) = V_{st}(r) + V_{ex}(r, E_i) + V_p(r, E_i) \tag{3}$$

where E_i is the incident energy. The three terms on the RHS of the Eq. (3) are various real potentials arising from the electron target interaction namely, static, exchange and the polarization potentials, respectively. The basic input for evaluating all these model potentials is the electronic charge density of the target. For atoms the charge density is derived from the parameterized Hartree–Fock wave functions given by Bunge and Barrientos [21]. However, for molecules the charge density is estimated by the following approximation. In general let us consider a molecule (halogen hydride) *AH*. Here it is convenient and useful to write the target (AH) charge density ρ_T in terms of atomic charge densities ρ_A and ρ_H as follows:

$$\rho_T = f_A\rho_A + f_H\rho_H \tag{4}$$

where f_A and f_H are the modulating factors obtained from the known values of the charge migrated to form the covalent bonding between the atoms *A* and *H*. This takes care of the bonding or overlap through partial charge transfer between the atoms in a molecule. The bond charges transferred partially to form the molecule *AH*, have been tabulated by Bader [22] in a number of simple cases. We employ the factors f_A and f_H in Eq. (4) so that it integrates to

$$N(T) = N(A) + N(H) \tag{5}$$

where $N(T)$ is the total number of electrons in AH_n, while $N(A)$ and $N(H)$ are the effective number of electrons for atoms *A* and H_n, respectively after the charge transfer. Thus we obtain the total renormalized charge density of the target *AH*.

The e–molecule system is more complex compared to e–atom system. In case of halogen hydrides our attempt is to reduce the system, to single centre by expanding the charge density of lighter hydrogen atoms at the centre of heavier halogen atom by employing the Bessel function expansion as in Gradshteyn and Ryzhik [23]. The molecular charge density $\rho(r)$, so obtained is renormalized to incorporate the covalent bonding. This has been employed earlier for many targets and is found successful in better representation of the target and hence predicting relevant cross sections [24,25]. This is a good assumption since it was observed that hydrogen atom does not significantly act as scattering centre and those cross sections were strongly affected by central atom size (see Fig. 9). We have then employed parameter free Hara's 'free electron gas exchange model' [26] for the exchange (V_{ex}) potential. All the target parameters, namely ionization potential, bond length and dipole polarizability of the target used in the calculation are the best available from the literature [27,28] and are given in Table 1.

Table 1
Target properties [27,28].

Target	IP (eV)	Bond Length (Å)
F	15.95	–
Cl	11.73	–
Br	11.81	–
I	10.45	–
HF	16.04	0.92
HCl	12.75	1.27
HBr	11.66	1.41
HI	10.39	1.61

The imaginary part in V_{opt}, also called the absorption potential V_{abs}, accounts for the total loss of scattered flux into all the allowed electronic channels of excitation and ionization. Here we have neglected the non-spherical terms arising from the vibrational and rotational excitation in the full expansion of the optical potential. This is due to the fact that anisotropic contribution from vibrational excitation will be significant at very low impact energies while it will be negligible at the energies of present interest. Moreover there is no contribution from rotational excitation since these hydrides do not possess permanent dipole moment.

Finally, for the absorption potential we have employed a well-known quasi-free model form of Staszewska et al. [29] given by

$$V_{abs}(r, E_i) = -\rho(r)\sqrt{\frac{T_{loc}}{2}} \cdot \left(\frac{8\pi}{10k_F^3E_i}\right)\theta(p^2 - k_F^2 - 2\Delta) \cdot (A_1 + A_2 + A_3) \tag{6}$$

The local kinetic energy of the incident electron is

$$T_{loc} = E_i - (V_{st} + V_{ex}) \tag{7}$$

The parameters A_1, A_2 and A_3 are defined as

$$A_1 = 5\frac{k_f^3}{2\Delta}; \qquad A_2 = \frac{k_f^3(5p^2 - 3k_f^2)}{(p^2 - k_f^2)^2};$$

$$A_3 = \frac{2\theta(2k_f^2 + 2\Delta - p^2)\cdot(2k_f^2 + 2\Delta - p^2)^{5/2}}{(p^2 - k_f^2)^2} \tag{8}$$

The absorption potential is not sensitive to long range potentials like V_{pol}. Hence it is not included in the representation of T_{loc} as shown in Eq. (7). In Eq. (6), $p^2 = 2E_i$, $k_F = [3\pi^2\rho(r)]^{1/3}$ is the Fermi wave vector and Δ is an energy parameter. Further $\theta(x)$ is the Heaviside unit step-function, such that $\theta(x) = 1$ for $x \geq 0$, and is zero otherwise. The dynamic functions A_1, A_2 and A_3 occurring in Eq. (6) depend differently on $\rho(r)$, I, Δ and E_i as evident from Eq. (8). The energy parameter Δ determines a threshold below which $V_{abs} = 0$, and the ionization or excitation is prevented energetically. In fact Δ is the governing factor which decides the values of total inelastic cross section and that is one of the characteristics of Staszewska model [29]. The original model of Staszewska et al. [29] has been modified by us by considering Δ as a slowly varying function of E_i around I. Briefly, a preliminary calculation for Q_{inel} is done with a fixed value $\Delta = I$. From this the value of incident energy at which our Q_{inel} reaches its peak, named as E_p is obtained. This is meaningful since Δ fixed at I would not allow excitation at incident energies $E_i \leq I$. On the other hand, if the parameter Δ is much less than the ionization threshold, then V_{abs} becomes unexpectedly high near the peak position. The modification introduced in our paper has been to assign a reasonable minimum value $0.8I$ to Δ and express this parameter as a function of E_i around I as follows:

$$\Delta(E_i) = 0.8I + \beta(E_i - I) \tag{9}$$

Here the value of the parameter β is obtained by requiring that $\Delta = I$ (eV) at $E_i = E_p$, beyond which Δ is held constant equal to I. The expression for $\Delta(E_i)$ is meaningful since Δ fixed at I would not allow excitation at incident energy $E_i \leq I$. On the other hand, if parameter Δ is much less than the ionization threshold, then V_{abs} becomes substantially high near the peak position. After generating the full complex potential given in Eq. (2) for a given electron–molecule system, we solve the Schrödinger equation numerically using partial wave analysis. At low energies only few partial waves are significant, e.g., at ionization threshold of the target around 5–6 partial waves are sufficient but as the incident energy increases more partial waves are needed. Using these partial waves the complex phase shifts are obtained which are employed to find the relevant cross sections vide Eq. (1) [20].

The two fundamental ingredients of the total cross sections as discussed earlier are the total elastic and total inelastic cross sections, which takes care of all the processes that result from the interaction of the incoming projectile with the target. Out of these two, the total inelastic cross section is solely responsible for the loss of incident flux in the out going channel. The loss can further be accounted mainly by two very important processes which are termed as ionization and sum of all electronic excitations. These processes are individually measurable and are reported in the literature as total ionization cross sections and partial or total excitation cross sections. But the sum of these two cross sections, i.e., the total inelastic cross section, Q_{inel}, cannot be measured directly in experiments, but can be estimated by subtracting total integral elastic cross section from the measured grand total cross sections. The measurable quantity of applied interest is the total ionization cross section, Q_{ion}, which is contained in the Q_{inel} which is rotationally and vibrationally elastic. The Q_{inel} can be partitioned into discrete and continuum contributions, viz.,

$$Q_{inel}(E_i) = \sum Q_{exc}(E_i) + Q_{ion}(E_i) \tag{10}$$

where the first term is the sum over total excitation cross sections for all accessible electronic transitions. The second term is the total cross section of all allowed ionization processes resulting in excitation to the continuum state induced by the incident electrons. The first term arises mainly from the low-lying dipole allowed transitions for which the cross section decreases rapidly at higher energies. The first term in Eq. (10), therefore becomes progressively smaller than the second at energies well above the ionization threshold. By definition,

$$Q_{inel}(E_i) \geq Q_{ion}(E_i) \tag{11}$$

In the present method Q_{ion} cannot be rigorously derived from Q_{inel} but may be estimated by defining the energy dependent ratio of cross sections,

$$R(E_i) = \frac{Q_{ion}(E_i)}{Q_{inel}(E_i)} \tag{12}$$

such that, $0 < R \lesssim 1$

We are required to impose three conditions on this dynamic ratio which has well justified physical footings. The conditions are summarized in the mathematical form through Eq. (13).

$$\begin{aligned} R(E_i) &= 0 \quad \text{for } E_i \leq I \\ &= R_P \quad \text{at } E_i = E_P \\ &\cong 1 \quad \text{for } E_i \gg E_P \end{aligned} \tag{13}$$

where 'E_p' stands for the incident energy at which the calculated Q_{inel} attains its maximum value. R_p is the value of R at $E_i = E_p$.

According to the first condition we require $R = 0$ when $E_i \leq I$. This is an exact condition as there is no ionization process possible if the incident energy is less than or equal to ionization threshold of the target. On the other hand the third condition is also physically justified that at very high incident energy, the only dominant inelastic channel is the ionization as the electronic excitation channels are almost over. So the ratio turns out to be nearly approaching one. Now the second condition is empirical in the sense that for a number of stable atoms and molecules like Ne, O_2, H_2O, CH_4, SiH_4, etc., for which the experimental cross sections Q_{ion} [30–32] are known accurately, the contribution of Q_{ion} is found to be about 70–80% of the total inelastic cross sections Q_{inel}. Here the upper bound is found only in rare case like that of Ne atom having an ionization potential of 21.56 eV. This behavior is attributed to the faster fall of the contribution of the first term $\sum Q_{exc}$ in Eq. (10) to the total inelastic cross sections, hence we choose $R_p = 0.7$. The lowest percentage is chosen here since the ionization potential of all the species studied here are in the range 10–16 eV as can be seen from Table 1. Also, choosing a single value will make our method consistent, predictive and reproducible. For calculating the Q_{ion} from Q_{inel} we need R as a continuous function of energy for $E_i > I$; hence we represent the ratio R in the following manner

$$R(E_i) = 1 - f(U) \tag{14}$$

Presently the above ratio has been determined using the following analytical form

$$R(E_i) = 1 - C_1\left(\frac{C_2}{U + a} + \frac{\ln(U)}{U}\right) \tag{15}$$

where U is the dimensionless variable defined by, $U = E_i/I$.

We have adopted this particular functional form for $f(U)$ in Eq. (15) due to its behavior with respect to the incident energy. As E_i increases above I, the ratio R increases and approaches unity, since the ionization contribution rises and the discrete excitation

Table 2
Various total ionization cross sections for halogens in Å^2.

E_i (eV)	F	Cl	Br	I
15	–	0.23	0.41	1.84
20	0.02	1.09	1.62	4.08
25	0.11	1.91	2.76	5.37
30	0.23	2.53	3.62	5.86
40	0.46	3.27	4.56	6.16
50	0.63	3.61	4.92	**6.23**
60	0.76	3.75	**4.97**	6.10
70	0.85	3.83	4.90	5.91
80	0.91	3.87	4.87	5.72
90	0.96	**3.88**	4.76	5.52
100	0.99	3.87	4.62	5.35
150	**1.03**	3.60	4.00	4.64
200	1.01	3.26	3.56	4.14
300	0.91	2.71	3.03	3.47
400	0.80	2.31	2.66	3.03
500	0.70	2.02	2.39	2.70
600	0.63	1.79	2.17	2.50
700	0.58	1.61	1.99	2.31
800	0.53	1.46	1.84	2.14
900	0.49	1.34	1.71	1.99
1000	0.45	1.23	1.61	1.87
2000	0.26	0.69	0.99	1.46

term in Eq. (10) decreases. The discrete excitation cross sections, dominated by dipole transitions, fall off as $\ln(U)/U$ at high energies. Accordingly the decrease of the function $f(U)$ must also be proportional to $\ln(U)/U$ in the high range of energy. However, the two-term representation of $f(U)$ given in Eq. (15) is more appropriate since the first term in the brackets ensures a better energy dependence at low and intermediate E_i. The dimensionless parameters C_1, C_2, and a, involved in Eq. (15) reflect the properties of the target under investigation. The three conditions stated in Eq. (13) are used to determine these three parameters and hence the ratio R. This is called the CSP-ic method. Having obtained Q_{ion} through CSP-ic method [2–4,18,19,24,25], the summed excitations cross sections $\sum Q_{exc}$ can be easily calculated vide Eq. (10).

3. Results and discussion

The theoretical approach of SCOP along with our CSP-ic method discussed above offers the determination of the total ionization cross sections, Q_{ion} along with a useful estimate on electronic excitations in terms of the summed cross section $\sum Q_{exc}$. Present data of total ionization sections results for the halogens and their halides are tabulated in Tables 2 and 3, respectively. Further, present results are also plotted and compared with available theoretical as well as experimental results through Figs. 1–8.

3.1. Halogen atoms (F, Cl, Br and I)

In Table 2 we have tabulated our results for the halogen atoms. The data given in the table as bold are the peak of Q_{ion} for each atom. It is well evident that the peak of the ionization cross section moves towards the low energy regime as the ionization potential decreases and the peak value of the cross section increases as the size of the target increases. This feature is a regular observation in most of the targets and thus gives a counter check to our theory.

A better understanding of the result may be obtained from the plots given below. In Fig. 1 we have depicted electron impact total ionization cross section for fluorine atom and compared with the existing data. The lone measurement of Q_{ion} for F atom is due to Hayes et al. [5] performed in the late eighties. They have quoted an uncertainty of about 20%, which is quite high to be considered as the recommended values. There are two previous theoretical results by Margreiter et al. [8] and Joshipura and Limbachiya [9]. Present

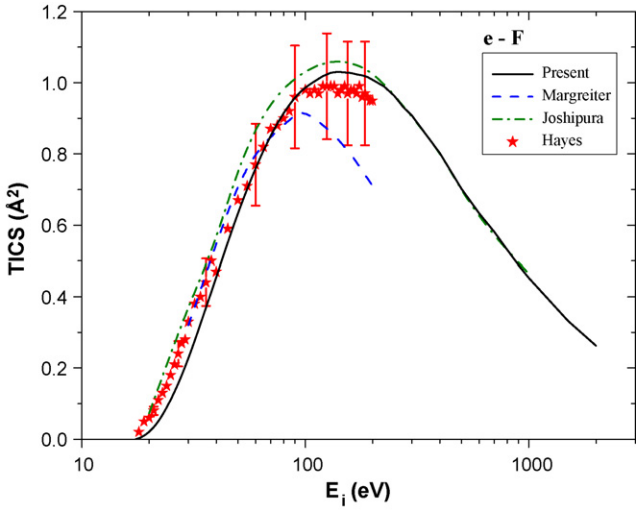

Fig. 1. Total ionization cross sections for e–F scattering in Å^2. Solid line, Present Q_{ion}; dash, Margreiter et al. [8]; dash-dot, Joshipura and Limbachiya [9]; stars, Hayes et al. [2].

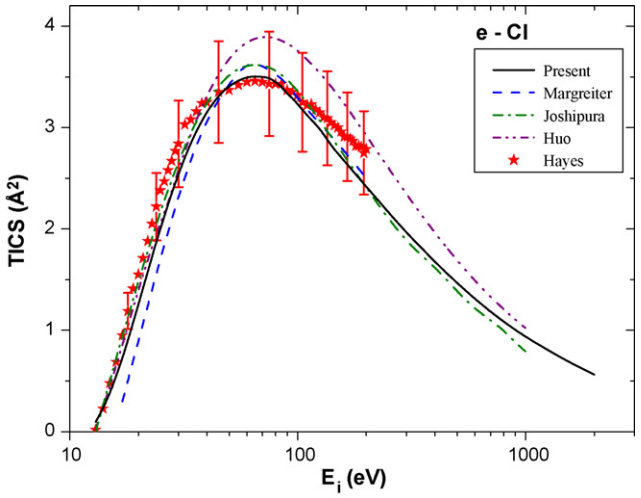

Fig. 2. Total ionization cross sections for e–Cl scattering in Å^2. Solid line, Present Q_{ion}; dash, Margreiter et al. [8]; dash-dot, Joshipura and Limbachiya [9]; dash-dot-dot, Huo [10]; stars, Hayes et al. [5].

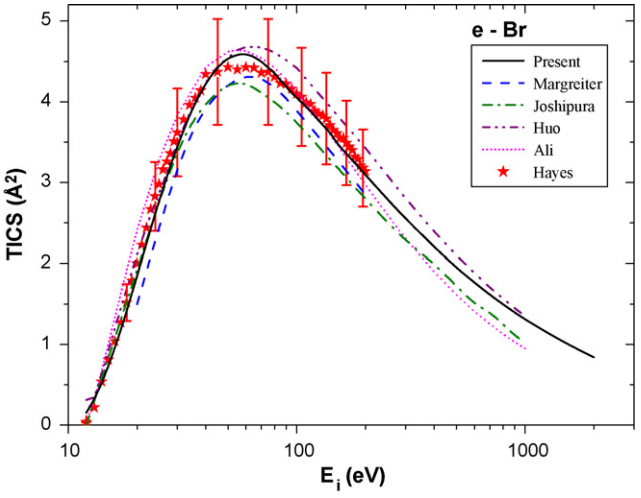

Fig. 3. Total ionization cross sections for e–Br scattering in Å^2. Solid line, Present Q_{ion}; dash, Margreiter et al. [8]; dash-dot, Joshipura and Limbachiya [9]; dash-dot-dot, Huo [10]; dot, Ali and Kim [7]; stars, Hayes et al. [5].

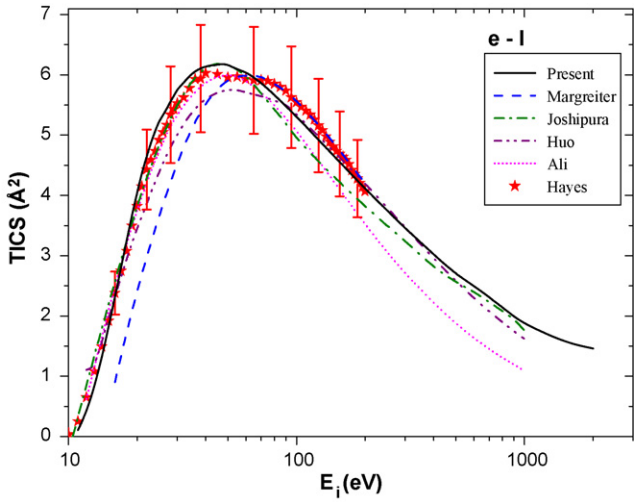

Fig. 4. Total ionization cross sections for e–I scattering in Å^2. Solid line, Present Q_{ion}; dash-dot, Joshipura and Limbachiya [9]; dash-dot-dot, Huo [10]; dot, Ali and Kim [7]; stars, Hayes et al. [5].

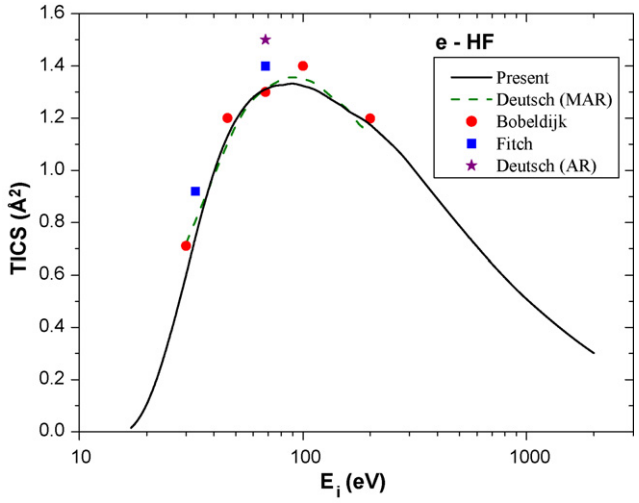

Fig. 5. Total ionization cross sections for e–HF scattering in Å^2. Solid line, Present Q_{ion}; dash, Deutsch et al. [11]; circle, Bobeldijk et al. [13]; square, Fitch and Sauter [12]; star, Deutsch and Schmidt [11].

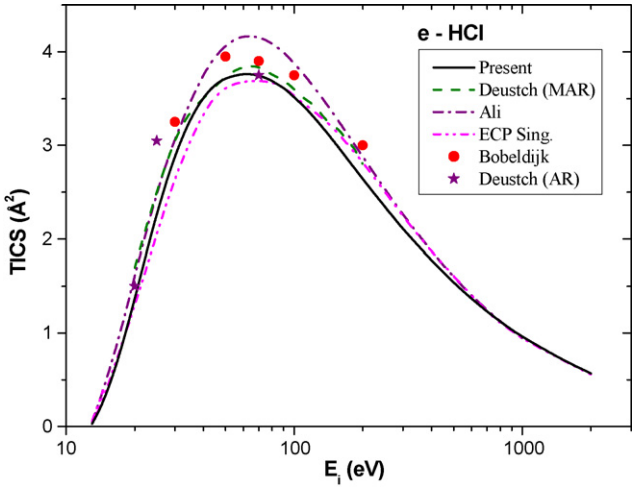

Fig. 6. Total ionization cross sections for e–HCl scattering in Å^2. Solid line, Present Q_{ion}; dash, Deutsch et al. [11]; dash-dot, Ali and Kim [7]; dash-dot-dot, ECP Sing. [7]; circle, Bobeldijk et al. [13]; star, Deutsch and Schmidt [11].

Table 3
Various total ionization cross sections for halogen hydrides in Å^2.

E_i (eV)	HF	HCl	HBr	HI
12	–	–	0.23	0.43
14	–	0.17	0.71	1.34
16	–	0.54	1.25	2.36
18	0.04	0.96	1.79	3.32
20	0.10	1.37	2.29	4.15
25	0.35	2.27	3.27	5.30
30	0.60	2.88	3.89	6.00
40	0.99	3.51	4.49	**6.47**
50	1.19	3.72	**4.65**	6.44
60	1.28	**3.76**	4.65	6.33
70	1.32	3.75	4.62	6.12
80	1.32	3.69	4.49	5.92
90	**1.33**	3.62	4.38	5.72
100	1.32	3.51	4.26	5.53
150	1.25	3.04	3.73	4.78
200	1.18	2.64	3.30	4.26
300	1.02	2.11	2.71	3.56
400	0.89	1.77	2.33	3.10
500	0.79	1.54	2.06	2.76
600	0.71	1.36	1.86	2.49
700	0.64	1.23	1.70	2.27
800	0.59	1.12	1.57	2.09
900	0.55	1.03	1.46	1.94
1000	0.51	0.96	1.37	1.82
2000	0.30	0.57	0.99	1.12

results are in excellent accord with the experiment [5] throughout the energy range and compares well with the theory of Joshipura and Limbachiya [9] except at the peak where they tend to be higher than all reported values. However, the values of Margreiter et al. [8] seem to fail beyond 80 eV.

Fig. 2 shows the comparison of present Q_{ion} for chlorine atom with the only measurement of Hayes et al. [5] and the theories of Margreiter et al. [8], Joshipura and Limbachiya [9] and Huo [10]. Present results finds very good comparison with measurement of Hayes et al. [5] and the theoretical results of Joshipura and Limbachiya [9]. The theoretical data of Huo [10] matches well with present data till 40 eV beyond which they are higher compared to all reported data, while the theories of Margreiter et al. [8] shows similar nature to all curves but are on the lower path. It is interesting to note that peak of ionization cross sections falls at same incident energy for all the data reported here.

We report our Q_{ion} for bromine atom along with the measurement of Hayes et al. [5] and theories of Margreiter et al. [8],

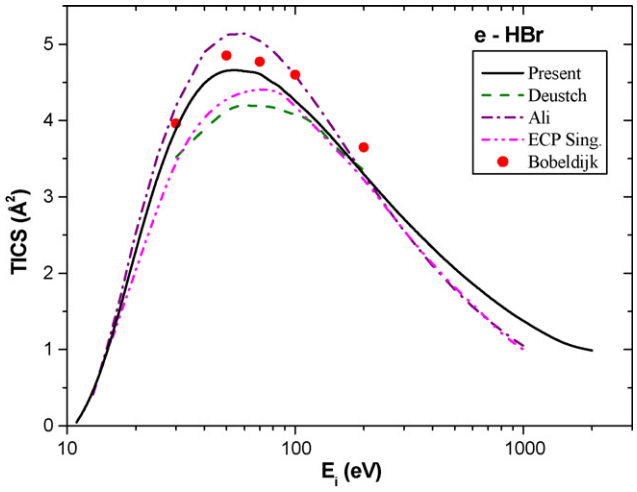

Fig. 7. Total ionization cross sections for e–HBr scattering in Å^2. Solid line, Present Q_{ion}; dash, Deutsch et al. [11]; dash-dot, Ali and Kim [7]; dash-dot-dot, ECP Sing. [7]; circle, Bobeldijk et al. [13].

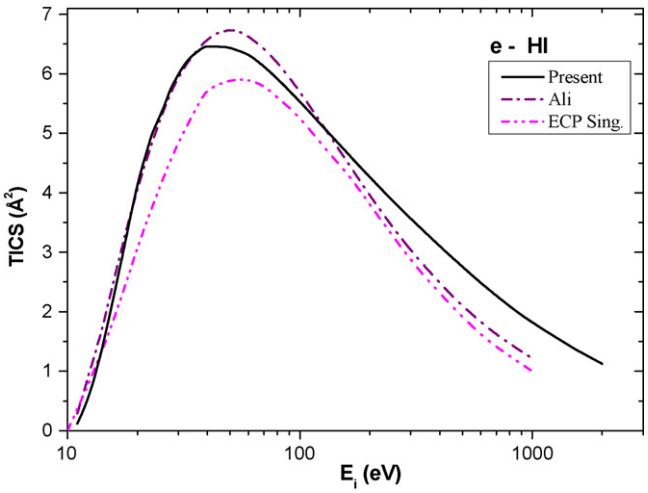

Fig. 8. Total ionization cross sections for e–HI scattering in Å^2. Solid line, Present Q_{ion}; dash-dot, Ali and Kim [7]; dash-dot-dot, ECP Sing. [7].

Joshipura and Limbachiya [9], Huo [10] and Ali and Kim [7] in Fig. 3. Our results find very good comparison with the measurements of Hayes et al. [5] over the entire range reported by them. Theoretical predictions of Ali and Kim [7] find very good agreement with present results till 200 eV beyond which they tend to diverge and are lower compared to our values. While the calculated data of Joshipura and Limbachiya [9] are in better agreement with present results till 30 eV beyond which they tend to be lower. Finally the theoretical data of Huo [10] show good accord with present results till 80 eV beyond which they are slightly higher than the present data.

Fig. 4 represents the comparison of the present total ionization cross sections for e – I scattering with other available data. As seen for earlier targets, in this case also there is an excellent agreement of present data with the measurement of Hayes et al. [5] and theoretical values of Huo [10] throughout the energy range reported by them. The theoretical predictions of Ali and Kim [7] goes very well with present results till 70 eV, above which they fall faster compared to all reported values. On the other hand the theoretical data reported by Margreiter et al. [8] are the lowest compared to all the data reported till 50 eV beyond which they merge with present results. Theoretical predictions of Joshipura and Limbachiya [9] show good accord with present data as well.

It is to be noted that present results goes in good accord with the measurements of Hayes et al. [5] for the entire range of incident energy reported by them, which is very encouraging since this feature is common in all the atomic species we have investigated here. This shows the consistency in our theory and gives us much confidence in calculating cross sections for other targets.

3.2. Halogen hydrides (HF, HCl, HBr and HI)

Table 3 gives present theoretical values of Q_{ion} calculated for the halogen hydrides from above ionization threshold to 2000 eV. The data given in the table as bold are the peak of Q_{ion} for each halogen hydride. A similar observation as that of halogen atoms vide Table 2 can be established here too. The peak of the ionization cross section seems to shift towards the lower energy side as the ionization potential of these targets decreases. Also, the value of its cross section at peak increases with the molecular size. Hence, the statement made for the atoms hold true for its hydrides as well.

Present Q_{ion} for HF is plotted and compared with available data in Fig. 5. In the absence of any measurement it becomes crucial to provide robust theoretical data to fill the gap in the database. However, previous theoretical data is very limited and perhaps for the first time the data is provided for such a wide range of energy. Deutsch et al. [11] have given their calculations using modified additivity rule in DM formalism for the incident energy 30–200 eV. There are some sample results (data points for few energies) provided using additivity rule by Fitch and Sauter [12] and Bobeldijk et al. [13]. The present results agree very well with theoretical data of Deustch et al. [11] and as expected the sample data of [12,13] are higher as they used additivity rule which generally overestimates at lower energy. Surprisingly there is no other comparison available from literature for this target. This may be due to its high volatile nature and hence very difficult to handle in the laboratories.

In our next figure (Fig. 6), we have plotted the Q_{ion} for HCl molecule and compared them with theoretical data of Deutsch et al. [11] and single ionization cross sections [7], and total ionization cross sections of Ali and Kim [7]. For this hydride also Fitch and Sauter [12] and Bobeldijk et al. [13] have provided their results for some of the sample energies. Present theory compares very well with the theoretical results of Deutsch et al. [11]. The sample results of Fitch and Sauter [12] and Bobeldijk et al. [13] calculated using AR are higher at low energies as expected and merges at energies above 100 eV showing the validity of additivity rule in this region. The single ionization cross sections represented as ECP method [7] are slightly lower compared to present data confirming the fact that single ionization is the most prominent process for this hydride. The total ionization cross sections given by Ali and Kim [7] are also in good accord with present data except at and near the peak, where they are slightly higher.

We have plotted in Fig. 7 the total ionization cross section for HBr molecule with the theoretical results of Deustch et al. [11], single and total ionization cross sections of Ali and Kim [7] and sample results of Bobeldijk et al. [13]. There is again no experimental data found in the literature for this hydride. All the theoretical data matches with present data till 25 eV, above which the data of Deutsch et al. [11] are slightly lower while that of Ali and Kim [7] are higher particularly near the peak region. The single ionization cross sections represented as ECP method are lower compared to present data as expected. The sample results of Bobeldijik et al. [13] are slightly higher since they have used additivity rule.

In our Fig. 8 we have plotted Q_{ion} for the HI molecule and compared it with the only theoretical data of single and total ionization cross sections of Ali and Kim [7]. The present data shows good accord with total ionization cross sections of Ali and Kim [7] calculated using BEB theory upto 30 eV above which they are slightly higher near the peak and then drops. The single ionization cross sections are lower as expected.

An interesting feature is observed in our last figure (Fig. 9) where we have plotted the Q_{ion} for both atoms and their hydrides. The cross section for each atom–atomic hydride pair seems to follow almost the same path. This aspect is very prominent in Br–HBr and I–HI pairs. One of the reasons may be due to the fact that their ionization potentials are comparable to each other. From Table 1 we find that the ionization potentials for Br–HBr pair (11.81 and 11.66 eV, respectively) and I–HI pair (10.45 and 10.39 eV, respectively) are close to each other and so are their cross sections. While for Cl–HCl pair the ionization potentials (11.73 and 12.75 eV, respectively) are 1 eV apart and hence the difference in cross sections. However, in case of H–HF pair, even though their ionization potentials (15.75 and 16.04 eV, respectively) are close enough, we find that their cross sections vary. This shows that not only ionization potential, but also their size matters. In the previous cases, the size of hydrogen atom was negligible to that of the halogen atom, and so hydrogen atom does not add much to the total cross sec-

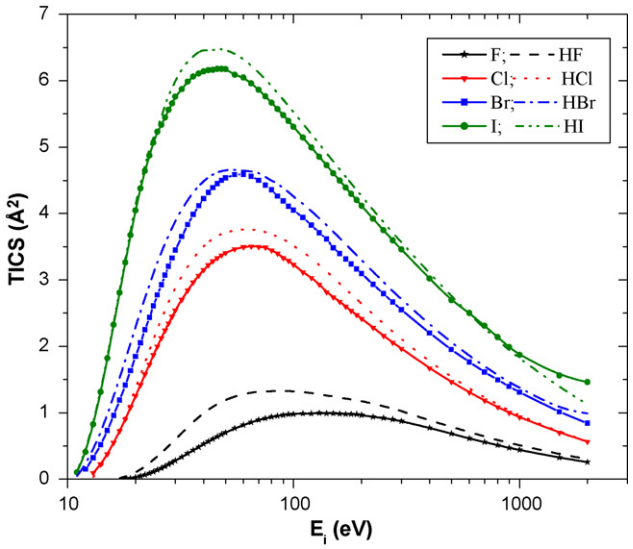

Fig. 9. Total ionization cross sections for all the targets in Å^2. Line with stars, F; dash, HF; line with inverted triangle, Cl; dot HCl, line with square, Br; dash-dot, HBr; line with circle, I; dash-dot-dot, HI.

tion. However, for the fluorine atom with atomic no. 9, the size of the hydrogen is comparable and hence the difference in the cross section.

4. Conclusion

A series of calculations to obtain total ionization cross sections for halogen atoms (F, Cl, Br and I) and halogen hydrides (HF, HCl, HBr and HI) were carried out. We have employed the well known SCOP and CSP-ic formalisms to perform these calculations. The results obtained are presented in the article and are compared with other available measurements and theories. Unavailability of required data set, especially reliable measurements make this study very imperative, since most of the previous studies are fragmented.

The results obtained for the halogen atoms are in good agreement with the available data. From Table 2 and Figs. 1–4, we can find that the result are very consistent in strength and shape and hence prove that present method can produce reliable cross sections even for the open shell systems.

In case of halogen hydrides, the observation is not that different (see Table 3 and Figs. 5–8). Overall, very good agreement between the various results can be seen from the graphs. A significant result for the molecules is that even after the bond formation with the hydrogen atom, the molecules gives quite similar cross section as that of the halogen atoms except in the case of HF. This may be attributed to the close proximity of ionization potential for atom-atomic hydride pair. Even though the ionization potential is similar in case of F and HF the cross sections are different since hydrogen atom also contributes comparable cross section as that of the F atom.

The values presented here can be considered reliable since the method employed here has been successfully tested for variety of targets from atoms to radicals and to heavier molecules [2–4,18,19,24,25]. In view of the fact that, present targets are halogen atoms and hydrides of these halogens, we are quite sure that the data presented here are consistent and can be further utilized to perform modeling in technological systems.

It is quite evident from the plots (Figs. 1–9) given in the previous section that present theory accounts for the ionization channel very well. The overall shape and strength of ionization cross section is nicely matched with measurements of Hayes et al. [5] for all the atoms studied here. This has given us the confidence in our calculation and hence we are convinced that present method can reproduce reliable cross section data for many more targets with adequate accuracy and speed. It is thus believed that such efforts will be more appreciated by the technology where cross section data is a necessary for further modeling of their systems. Also, we hope that our effort will encourage experimentalists to perform more measurements of these important targets.

Acknowledgement

MVK is thankful to University Grants Commission New Delhi, for Major Research Project under which part of this work is carried out.

References

[1] W.L. Morgan, Plasma Chem. Plasma Process. 12 (1992) 449–476.
[2] M. Vinodkumar, C. Limbachiya, B. Antony, K.N. Joshipura, J. Phys. B: At. Mol. Opt. Phys. 40 (2007) 3259.
[3] M. Vinodkumar, K.N. Joshipura, C. Limbachiya, N. Mason, Phys. Rev. A 74 (2006) 022721.
[4] M. Vinodkumar, C. Limbachiya, K. Korot, K.N. Joshipura, N. Mason, Int. J. Mass Spectrom. 273 (2008) 145.
[5] T.R. Hayes, R.C. Wetzel, R.C. Freund, Phys. Rev. A 35 (1987) 578.
[6] R.S. Freund, R.C. Wetzel, R.J. Shul, T.R. Hayes, Phys. Rev. A 41 (1990) 3575.
[7] M.A. Ali, Y.-K. Kim, J. Phys. B: At. Mol. Opt. Phys. 41 (2008) 145202.
[8] D. Margreiter, H. Deustch, T.D. Märk, Int. J. Mass Spectrom. Ion Proc. 139 (1994) 127.
[9] K.N. Joshipura, C.G. Limbachiya, Int. J. Mass Spectrom. 216 (2002) 239.
[10] W. Huo, NASA website: http://www.ipt.arc.nasa.gov/databasemenu.html.
[11] H. Deutsch, K. Becker, T.D. Märk, Int. J. Mass Spectrom. Ion Proc. 167/168 (1997) 503.
[12] W.L. Fitch, A.D. Sauter, Ann. Chem. 55 (1983) 832.
[13] M. Bobeldijk, W.J. van der Zande, P.G. Kistemaker, Chem. Phys. 179 (1994) 125.
[14] W. Huo, Y.-K. Kim, Chem. Phys. Lett. 319 (2000) 516.
[15] A. Jain, K.L. Baluja, Phys. Rev. A 45 (1992) 202.
[16] A. Jain, Phys. Rev. A 34 (1986) 3707.
[17] A. Jain, J. Phys. B 22 (1988) 905.
[18] K.N. Joshipura, M. Vinodkumar, C.G. Limbachiya, B.K. Antony, Phys. Rev. A 69 (2004) 022705.
[19] M. Vinodkumar, C. Limbachiya, K.N. Joshipura, B. Vaishnav, S. Gangopadhayay, J. Phys. Con. Series 115 (2008) 012013.
[20] C.J. Joachain, Quantum Collision Theory, North-Holland, 1983.
[21] C.F. Bunge, J.A. Barrientos, At. Data Nucl. Data Tables 53 (1993) 113.
[22] R.F.W. Bader, Atoms in Molecules: A Quantum Theory, Clarendon Press, Oxford, 1990.
[23] I. Gradshteyn, I.M. Ryzhik, Tables of Integrals, Series and Products, Associated Press, New York, 1980.
[24] M. Vinodkumar, C. Limbachiya, K. Korot, K.N. Joshipura, Eur. Phys. J. D 48 (2008) 333.
[25] M. Vinodkumar, K.N. Joshipura, C.G. Limbachiya, B.K. Antony, Eur. Phys. J. D 37 (2006) 67.
[26] S. Hara, J. Phys. Soc. Jpn. 22 (1967) 710.
[27] D.R. Lide, CRC Handbook of Physics and Chemistry, 74th ed., Chemical Rubber Company, Boca Raton, FL, 1993–1994.
[28] From: http://srdata.nist.gov/cccbdb/.
[29] G. Staszewska, D.W. Schwenke, D. Thirumalai, D.G. Truhlar, Phys. Rev. A 28 (1983) 2740.
[30] R. Basner, M. Schmidt, V. Tarnovsky, K. Becker, Int. J. Mass Spectrom. Ion Proc. 171 (1997) 83.
[31] E. Krishnakumar, S.K. Srivastava, J. Phys. B 21 (1988) 1055.
[32] G.P. Karwasz, R.S. Brusa, A. Zecca, Riv. Nuovo Cimento 24 (1) (2001) 1.